Proceedings of the 2002 IEEE International
Conference on Control Applications
September 18-20.2002 • Glasgow, Scotland, UX

VISION BASED CONTROLLER FOR AUTONOMOUS AERIAL REFUELING

Jennifer Kimmett, John Valasek, and John L. Junkins
Aerospace Engineering Department
Texas A&M University, College Station, TX 77843-3141
http://jungfrau.tamu.edu/-htmllvalasek

1. A13STRACT

Autonomous aerial refueling is an important capability for unmanned aerial vehicles. This paper develops a candidate autonomous probe-and-drogue aerial refueling controller for an existing vision based relative position sensor and navigation system. Feasibility of the combined sensor-navigator-controller is demonstrated by a simulated UAV docking maneuver to a moving drogue, in light turbulence. Results indicate that the controller can provide precise aerial refueling with good disturbance rejection characteristics.

2. INTRODUCTION

Autonomous Aerial Refueling (AAR) is the best solution to increasing the endurance of Unmanned Aerial Vehicles (UAVs), since endurance can be increased significantly without having to trade-off payload and range [1]. The probe-and-drogue refueling system is the standard for the United States Navy and the air forces of many nations. In this method, the tanker trails a hose with a flexible "basket" at its end called a paradrogue, and the pilot of the receiver aircraft must maneuver to place the receiver's probe into the paradrogue (Figure 1).

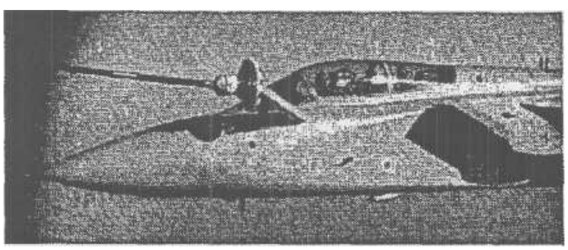

Figure 1. GR-1 Tornado Refueling
Using the Probe-and-Drogue Method

It is essentially a high precision docking operation requiring 0.5 to 1.0 cm accuracy in the relative position of the receiving aircraft with respect to the paradrogue.

For the past five years the Vision Navigation Laboratory at Texas A&M University has been developing a novel vision based sensor and relative navigation system that has very high accuracy, called VisNav [2]. VisNav has been applied to the problem of spacecraft formation flying [3], and AAR of UAVs [4]. Probe-and-drogue refueling is also a high gain task, and excessive control rates can lead to Pilot Induced Oscillations (PIO) 151. Reference 6 developed a VisNav based AAR controller which suppressed control rates by pre-filtering control commands with a low pass filter, that was tuned with quadratic weights. It was combined with a Kalman filter state estimator, and used to track a stationary paradrogue from initial position offsets. Simulations with process and sensor measurement noise, with moderate turbulence, produced good results.

This paper extends the controller of [6] by mating it to a discrete version of the explicit model following Command Generator Tracker (CGT) of reference [7], thereby enabling the controller to track the time-varying motions of a non-stationary paradrogue. A simulation test case of this controller tracking a non-stationary paradrogue in light turbulence is presented.

3. DISCRETE PIF-CGT CONTROLLER

Consider the state-space representations of a discretized linear time-invariant continuous plant with n states and m controls

$$x_{k+1} = \Phi x_k + \Gamma u_k \; ; \qquad x_0 = x0$$
$$y_k = Hx_k + Du_k \tag{1}$$

$$x_k \in R^n,\ u_k \in R^m,\ y_k \in R^m$$
$$\Phi \in R^{n \times n},\ \Gamma \in R^{n \times m},\ H \in R^{m \times n},\ D \in R^{m \times m}$$

and a user specified discrete linear time-invariant model with l states and m controls

$$x_{m_{k+1}} = \Phi_m x_{m_k} + \Gamma_m u_{m_k}$$
$$y_{m_k} = H_m x_{m_k} + D_m u_{m_k} \tag{2}$$

$$x_m \in R^l,\ u_m \in R^m,\ y_m \in R^m$$
$$\Phi_m \in R^{l \times l},\ \Gamma_m \in R^{l \times m},\ H_m \in R^{m \times l},\ D_m \in R^{m \times m}$$

All

The CGT is an explicit model following control technique in which user specified output trajectories of the plant are forced to track the output trajectories of a specified model system. The sampled-data version is derived here. The problem statement is to determine the admissible control sequence of the continuous plant input with zero-order hold **u(t) -** u_k, $kT \leq t < (k+1)T$ that will drive the plant output sequence $y_k = y(kT)$ to exactly track the model output sequence $y_{jk} = y_m(kT)$. Throughout this derivation quantities denoted by the superscript * represent the desired state and control trajectories to be tracked. Thus when $y_r = y_m$, the states and controls will be at $x_k = x$, and $u_k = u_k$.

A discrete state-space representation of the errors between the actual and desired trajectories in PIF format is developed first. For Type I tracking, integral action is applied to the error between the actual and commanded outputs y_{1k}, so that

$$Y_{I} = \sim(Y_k - Y_{.})$$

Taking the derivative of both sides produces the state equation for the error of the integrated states,

$$Y_{I_{k+1}} = Y_{I_k} + T(Y_k - Y_{r,k}) \qquad (3)$$

where $y_{1k} \in R^m$ and T is the sample period. The errors between the actual and desired state and control trajectories are defined as

$$\begin{aligned} x_k &= x_k - x_k \\ U_k &= U_k - U_k \end{aligned} \qquad (4)$$

An expression for (3) in terms of the trajectory errors is obtained by substituting (4) into (1), resulting in

$$Y_{I_{k+1}} = Y_{I_k} + T(Hx_k + Du_k) \qquad (5)$$

Excessive control rates are suppressed by pre-filtering the controls. This is done by making the control inputs U_k a system state, and the control rates, denoted by $u_{r,k}$, the inputs to the system. The result is the first-order pre-filter on the controls

$$U_{k+1} = U_k + Tu_{1,k} \qquad (6)$$

Converting to error quantities,

$$U_{k+1} = d_k + Tu_{r,k} \qquad (7)$$

The combined discrete state-space system composed of the state errors, pre-filtered controls, and commanded output errors is represented by

$$\tilde{x}_{I_{k+1}} = \begin{bmatrix} x_{k+1} \\ \tilde{u}_{k+1} \\ y_{I_{k+1}} \end{bmatrix} = \begin{bmatrix} \Phi & \Gamma & 0 \\ 0 & 1 & 0 \\ TH & TD & I \end{bmatrix} \begin{bmatrix} x_k \\ U_k \\ Y_{I_k} \end{bmatrix} + \begin{bmatrix} 0 \\ TI \\ 0 \end{bmatrix} u_{r,k} \qquad (8)$$

The sampled-data regulator of [8] is used to obtain optimal tracking gains. The associated cost function to be minimized for (8) has the form

$$J = \frac{1}{2}\sum^{\infty} [\tilde{x}_{I_k}^T \hat{Q} \tilde{x}_{I_k} + u^T \hat{R} u_{r,k} + 2\tilde{x}_{I_k}^T \hat{M} u_{r,k}] \qquad (9)$$

in which $\hat{Q}$ is the discrete equivalent of the continuous matrix Q which weights error states, error controls, and error of integrated states, and $\hat{R}$ is the discrete equivalent of the continuous control rate weighting matrix R. $\hat{M}$ results from the discretization process. It can be easily shown that the feedback control policy which minimizes (9) is negative feedback of all the states. For the present controller, this results in

$$u_{r,k} = U_{1,k} - U_{r,k} = -K_1 x_k - K_2 u_k - K_3 Y_{I_k} \qquad (10)$$

and the feedback gains are calculated by solving a matrix Ricatti equation [8]. Re-writing (10) in terms of the measured state and control vectors, and the commanded state and control vectors, results in the PIF feedback control law

$$u_{r,k} = (u_{r,k} + K_1 x_k + K_2 u_k) - K_1 x_k - K_2 u_k - K_3 Y_{I_k} \qquad (11)$$

where all * quantities are to be determined, and must ultimately be expressed in terms of model states and controls. The required expressions are obtained from the discrete CGT as follows. Recognizing that the discretized state and output equations in steady-state must satisfy

$$\begin{cases} \ldots \\ Y_k{}' \sim - CH \end{cases} \begin{bmatrix} \Gamma \\ D \end{bmatrix} \begin{bmatrix} x_k^* \\ u_k^* \end{bmatrix}$$

a constant matrix

$$A, \begin{bmatrix} A_{11} & A_{12} \\ A_{21} & A_{22} \end{bmatrix}; \quad \in \sim(n+m)\times(l+m)$$

is used to define the needed mapping from model states and controls, to the desired states and controls:

$$X:] = [-I \quad 42][^{x} -.k]$$
$$n_k \quad A,: \quad An ..,k$$

To obtain a closed-form solution, the model control rates are assumed to be zero, i.e. the model controls are held constant. The effect of this assumption is that perfect tracking of time varying model outputs is achieved only when the model control rates are zero, which only occurs in steady-state. However, even when the model control rates are nonzero, experience has shown this controller to provide excellent tracking. Incrementing (13) and applying the model controls assumption results in

$$rXk+, -a'[-CA_n \quad 41 \quad 42 \quad xA.k+, -am.k \tag{14}$$
$$L\dot{U}k+, - Uk \quad 4211$$

Substituting the model state and output equations from (2) into (14),

$$xk+, - xk \;] = CA.. (()m -1) \quad Air. lr\, U.k\sim$$
$$1 \quad Yk \quad H_m \quad J \quad m$$

Subtracting xk from both sides of (12) and transforming the desired states and controls into the model states and controls through the linear mapping in (13) results in

$$Yk+,-xr1=C(c-1) \quad D11\text{-}4 \quad Al211^{x} m,k \tag{16}$$
$$C \quad yk \quad H \quad 21 \quad A_n \quad u_m \quad J$$

Equating (IS) and (16) finally produces the linear mapping between the desired states and controls, and the model states and controls:

$$\sim A, \quad 4_2 1 \quad [((D^{-1}) \quad r$$
$$A_I, \quad A22 \quad H \quad DI$$
$$+ A_{ll} (\sim_m - 1) A_l, r_m$$
$$Hm \quad D$$

The only unknowns are the A, . The first matrix on the right hand side of (17) is the inverse of a Quad Partition Matrix (QPM), with redefined elements

$$[(cF -1) \quad r \quad - \sim\sim 1, \quad nl21$$
$$H \quad D1 \quad -[X21 \quad X22$$

The QPM substituted into (17) and produces a set of equations for A,, . The first equation is a non-symmetric Lyapunov equation, whose solution exists provided no plant eigenvalues are canceled by a transmission zero.

Once A,, is known, all of the other A_{ii} terms are determined by direct substitution:

$$A, = n \, 41 \, ('m-1)+rr,2H,$$
$$A,2 = lr,, \, 4, r_m + rr_{12} D$$
$$A21 = T2, A\, 1\, (0m^{-1}) + n22\, H_m$$
$$4_2 = ;r_{2l} A\, lrm + 1r_2 D_m$$

With $A_{;i}$ determined, the desired controls in (13) can now be solved for. To get them (6) is re-arranged and expressed in the notation

$$u^{\bullet}, = -(u_{k+1} - u)$$

An expression for (18) in terms of model states and model controls is obtained by substituting the bottom row of (14) and then the model state equation of (2). After collecting terms,

$$u;, = \quad [(cm^{-1})zm,+rmum,J$$

Finally, substituting the desired states and controls (13) and desired control rates (19) into the discrete PIF control law (11) produces the desired result:

$$u_{,+} = [K.A_l + K_2 4, + -((D.^{-1})]\, _{m,}$$
$$+[K_1 A_{12} + K_2 A_{22} + \mathcal{I}^{L} r_m] u_m, \tag{20}$$
$$-K, z_k - K_2 u_k - K, y,,$$

The resulting discrete PIF-CGT controller requires measurement and feedback of the plant states, plant controls, and integrated states. It also requires that the model states and model controls be fed forward. Whereas the constant terms in the A, matrix can be calculated a-priori, the non-stationary compensator of the model system must be evaluated online during each computation cycle. For the PIF-CGT control policy to be admissible, the quad partition matrix must be invertible. This restricts the number of commanded outputs to the number of available plant controls. Additionally, no model eigenvalues may coincide with any plant transmission zeros.

4. CONTROLLER INPUTS AND ESTIMATES

The discrete PIF-CGT controller receives six degree-of-freedom paradrogue position and attitude inputs from the VisNav sensor via a Gaussian Least Squares Differential Correction (GLSDC) algorithm. A Variational Kalman Filter (VKF) is designed to handle uncertainties in the plant, filter exogenous inputs (such as turbulence and gusts), and filter measurement noise from the sensors used for the non-VisNav supplied measurements. It also estimates the controller states not provided by the GLSDC. Each of these algorithms were developed in detail in [6], and are used again here.

5. PARADROGUE DYNAMICS

The lateral and vertical positions of the paradrogue oscillate because of wing tip vortices shed from the tanker aircraft, since the Buddy Store which houses the paradrogue is mounted on the tanker's wing. Additionally, the paradrogue tends to translate horizontally with a perturbation velocity. Simple longitudinal and lateral/directional models of these effects are used here in the simulation model. The paradrogue longitudinal dynamical model is

$$\begin{bmatrix}\dot x_d\\ \dot z_d\\ \ddot z_d\end{bmatrix} = \begin{bmatrix}0&0&0\\0&0&1\\0&-w_z&0\end{bmatrix}\begin{bmatrix}x_d\\ z_d\\ \dot z_d\end{bmatrix} + \begin{bmatrix}u_d&0\\0&0\\0&0\end{bmatrix}\begin{bmatrix}\delta x_s\\ \delta z_s\end{bmatrix}$$

where all d subscripts refer to a paradrogue body-fixed axis system. The perturbed horizontal paradrogue velocity u_d is set to a value of 5 feet/sec, and the vertical oscillation frequency w_z is set to a value of 0.3162 Hz. The input to the horizontal component is a unit step, and a step input to the vertical component controls the perturbation altitude that the paradrogue oscillates about. The paradrogue longitudinal output equation is

$$\begin{bmatrix}x_d\\ z_d\end{bmatrix} = \begin{bmatrix}1&0&0\\0&1&0\end{bmatrix}\begin{bmatrix}x_d\\ z_d\\ \dot z_d\end{bmatrix} + \begin{bmatrix}0&0\\0&1\end{bmatrix}\begin{bmatrix}\delta x_s\\ \delta z_s\end{bmatrix} \qquad (22)$$

Similarly, the lateral/directional dynamical model of the paradrogue is an undamped oscillator with frequency ω_y, set to a value of 0.3162 Hz. The magnitude of the step input to the lateral equation controls the lateral perturbation position that the paradrogue oscillates about. The paradrogue lateral/directional dynamical model is

$$\begin{bmatrix}\dot y_d\\ \ddot y_d\end{bmatrix} = \begin{bmatrix}0&1\\-w_y&0\end{bmatrix}\begin{bmatrix}y_d\\ \dot y_d\end{bmatrix} + \begin{bmatrix}0\\1\end{bmatrix}\delta y_s \qquad (23)$$

and the paradrogue lateral/directional output equation is

$$y_d = \begin{bmatrix}1&0\end{bmatrix}\begin{bmatrix}y_d\\ \dot y_d\end{bmatrix} + [1]\,\delta y_s \qquad (24)$$

6. UAV CONTROL AND SIMULATION MODEL

The UAV model used for controller design and simulation is called UCAV6. The UCAV6 simulation was developed in 1997 at Texas A&M University with the help of Engineering Systems, Inc. as part of an Office of Naval Research Uninhabited Combat Air Vehicle (UCAV) research program. It is a roughly 60% scale AV-8B Harrier aircraft, with the pilot and support devices removed and the mass properties adjusted accordingly [9]. The UCAV6 simulation is a nonlinear, non real-time, six-degree-of-freedom computer code written in Microsoft Visual C++ 5.0. The full-order linearized UCAV6 longitudinal and lateral/directional models used in this paper were obtained from the UCAV6 simulation [10].

7. NUMERICAL EXAMPLE

The control objective is to dock the tip position of the refueling probe with a moving paradrogue, with an accuracy of 1.0 cm and a docking speed less than 10 feet/sec. The VisNav sensor is positioned on the surface of the UAV, slightly aft and to the side of the refueling probe. The flight condition is 250 KTAS at an altitude of 20,000 feet, and the initial position of the drogue is 100 feet in front, 50 feet above, and 50 feet to the left of the initial trimmed position of the UAV. Dryden light turbulence (sigma = 2.5 for this flight condition) is present, and affects both the drogue and the UAV.

The basic CGT structure permits a number of commanded plant outputs equal to the number of controls. With four controls, the controller commands the UAV to the time-varying drogue position (x_d, y_d, z_d), and commands yaw attitude angle. The sample period is T = 0.1 seconds for all sub-systems in the combined system. Process noise of N(0,0.01) is applied to all longitudinal and lateral/directional states except for the body-axis velocities, which use the turbulence intensity. The VKF uses process noise of N(0,E-7) applied to all states, and measurement noise of N(0,0.01) on the states and N(0,0.1) on the controls.

Figure 2 shows the trajectory of the probe tip in blue, starting from the origin, and the trajectory of the oscillating paradrogue in red. After reducing the relative position errors to near zero (Figure 3), the probe is close but does not successfully dock, according to the criteria of simultaneous zero relative position errors. This is because the model states and controls which represent the paradrogue motions are not measurements, but internal states of the PIF-CGT controller. Thus they are not process noise filtered by the VKF like the receiver UAV state measurements are. For test cases without turbulence, the probe was shown to easily dock with the paradrogue even though it was oscillating. Figure 3 also shows that the inertial attitude angles are all within acceptable limits.

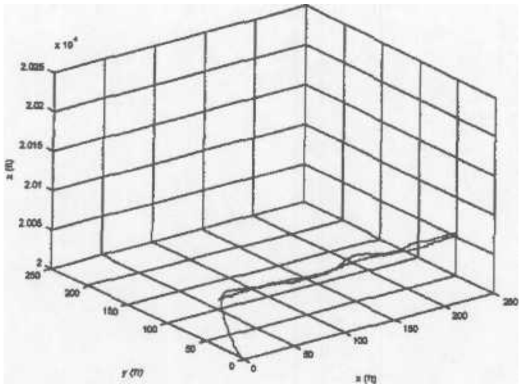

Figure 2. Probe Tip and Paradrogue Trajectories

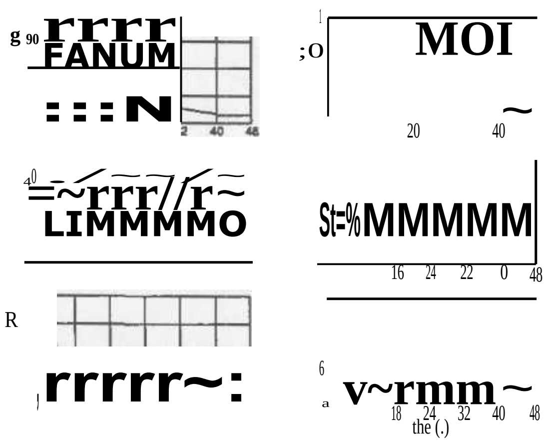

Figure 3. Relative Position Errors Between
Probe Tip and Paradrogue, and Attitude Angles

Figure 4 shows the body-axis velocities of the receiver UAV including the induced gust velocities. Note that the probe approach speed is well below 10 feet/sec, as desired. Estimates of the body-axis velocities and positions from the VKF are shown as the dashed green line in each plot. The agreement is seen to be excellent, particularly for the probe positions.

Figure 5 shows that angle-of-attack and sideslip angle are well damped, and the excursions are within acceptable limits. The same can be seen for the body-axis rates.

The control effectors and control rates are shown in Figure 6. The throttle is advanced to provide more power as the receiver UAV climbs toward the paradrogue, and is then throttled back to the original trim setting of 55% upon closing with the drogue, as desired. The desired low-pass filtering effect of the PIF-CGT on the controls is evident, as each is smooth and exhibits positions and rates below the limits for this class of vehicle by at least a factor of 20.

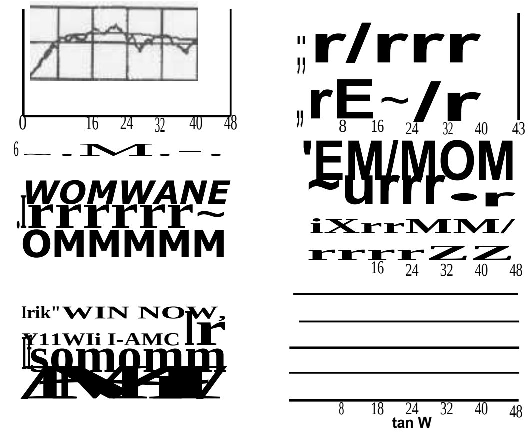

Figure 4. Body-Axis Velocities and Probe Positions

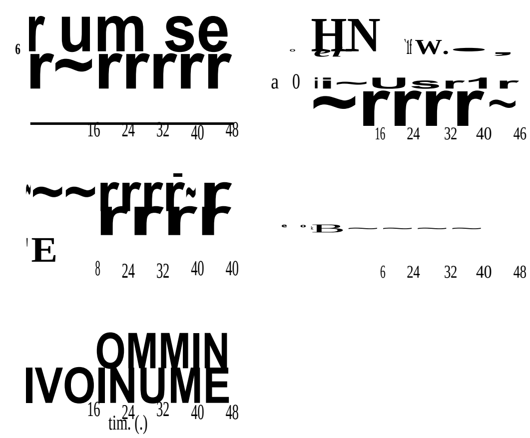

Figure 5. Body-Axis Rates,
Angle-of-Attack, and Sideslip Angle

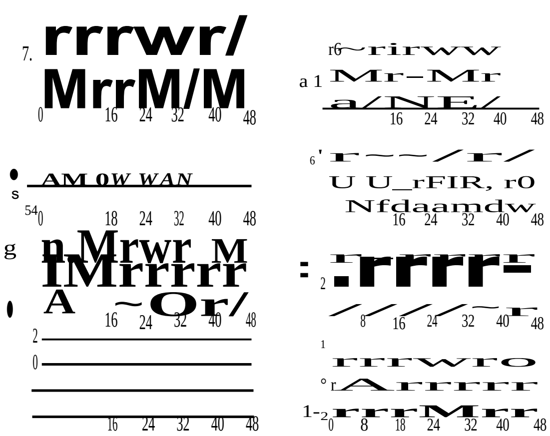

Figure 8. Control Position and Rate Time Histories

8. CONCLUSIONS AND FURTHER WORK

This paper presented a candidate controller for a vision based autonomous aerial refueling system. A discrete Proportional Integral Filter - Command Generator Tracker controller was derived, that has Type I tracking, permits control rates to be weighted by the designer, and uses an explicit model of the desired tracking dynamics. A Variational Kalman Filter was designed and implemented to estimate required controller feedback states and to filter noisy measurements. The controller was then integrated with an existing vision based sensor and associated Gaussian Least Squares Differential Correction algorithm, which provides the navigation solution and relative position and attitude estimates to the controller. Performance of the controller was evaluated by a simulation test case of a receiver UAV probe-and-drogue docking maneuver with an oscillating drogue, from an initial position offset, in the presence of atmospheric turbulence. Results demonstrated that the controller is able to guide the probe very close to the oscillating drogue, but cannot achieve a complete docking due to turbulence effects on the paradrogue that the controller is not designed to handle. Repeating the case in still air resulted in a complete docking with the oscillating probe. Overall the system performed well as no large excursions in the states occurred, and control deflections, rates, and effort were well under limits.

Further investigations will extend the controller structure to filter process noise on the paradrogue, improve the overall disturbance rejection properties, and employ more detailed and accurate sensor and measurement models.

9. ACKNOWLEDGMENTS

This research is funded by a National Defense Science and Engineering Graduate Fellowship in conjunction with the Army Research Office, by the State of Texas Advanced Technology Program, and by Zonta International Women's Organization. This support is gratefully acknowledged by the authors.

10. REFERENCES

[1] Woodward, William E., "The Future of Unmanned Aerial Vehicles in U.S. Military Operations," International Security and Economic Policy Specialization Project, Maryland School of Public Affairs, May 2000.

[2] Junkins, John L., Hughes, Declan, Wazni, Karim, and Pariyapong, Vatee, "Vision-Based Navigation for Rendezvous, Docking, and Proximity Operations," ASS-99-021, *22nd Annual ASS Guidance and Control Conference,* Breckenridge, Colorado, February 1999.

[3] Alonso, Roberto, Crassidis, John L., and Junkins, John L., "Vision-Based Relative Navigation for Formation Flying of Spacecraft," AIAA-2000-4439, *American Institute of Aeronautics and Astronautics,* 2000.

[4] Valasek, John, Kimmett, Jennifer, Hughes, Declan, Gunnam, Kiran, and Junkins, John L., "Vision Based Sensor and Navigation System for Autonomous Aerial Refueling," AIAA-2002-3441, Proceedings of the First AIAA Conference and Workshop on Unmanned Aerospace Vehicles, Systems, Technologies, and Operations, Portsmouth, VA, 12-14 May 2002.

[5] Klyde, D. H., D. G. Mitchell, and K. J. Latimer, "Development of the Probe-and-Drogue Handling Qualities Demonstration Maneuver," *Journal of Guidance, Control, and Dynamics,* Vol. 22, No. 4, July - Aug. 1999.

[6] Kimmett, Jennifer, Valasek, John, and Junkins, John L., "Autonomous Aerial Refueling Utilizing a Vision Based Navigation System," AIAA-2002-4469, Proceedings of the AIAA Guidance, Navigation and Control Conference, Monterey, CA, 5-8 August 2002.

[7] Lewis, Frank L., **Applied** Optimal Control & Estimation, Prentice Hall, Englewood Cliffs, N.J., 1992, pp. 234-245.

[8] Dorato, P., and Levis, A.H., "Optimal Linear Regulators: The Discrete-Time Case," *IEEE Transactions on Automatic Control,* Vol. AC-16, No. 6, December 1971, pp. 613-620.

[9] Smith, David M., and Valasek, John, "Agility Metric Robustness Using Linear Error Theory," *Journal of Guidance, Control, and Dynamics,* Vol. 24, No. 2, pp. 340-351, March-April 2001.

[10] Texas A&M University, Flight Simulation Laboratory, Unmanned Combat Aerial Vehicle (UCAV) Modeling website, http://aerounix.tamu.edu/ueav